# Tropical Cyclone Lightning and Rapid Intensity Change

MARK DeMARIA

*NOAA/NESDIS/STAR, Fort Collins, Colorado*

ROBERT T. DeMARIA

*CIRA/Colorado State University, Fort Collins, Colorado*

JOHN A. KNAFF AND DEBRA MOLENAR

*NOAA/NESDIS/STAR, Fort Collins, Colorado*

ABSTRACT

A large sample of Atlantic and eastern North Pacific tropical cyclone cases (2005–10) is used to investigate the relationships between lightning activity and intensity changes for storms over water. The lightning data are obtained from the ground-based World Wide Lightning Location Network (WWLLN). The results generally confirm those from previous studies: the average lightning density (strikes per unit area and time) decreases with radius from the storm center; tropical storms tend to have more lightning than hurricanes; intensifying storms tend to have greater lightning density than weakening cyclones; and the lightning density for individual cyclones is very episodic. Results also show that Atlantic tropical cyclones tend to have greater lightning density than east Pacific storms. The largest lightning density values are associated with sheared cyclones that do not intensify very much. The results also show that when the lightning density is compared with intensity change in the subsequent 24 h, Atlantic cyclones that rapidly weaken have a larger inner-core (0–100 km) lightning density than those that rapidly intensify. Thus, large inner-core lightning outbreaks are sometimes a signal that an intensification period is coming to an end. Conversely, the lightning density in the rainband regions (200–300 km) is higher for those cyclones that rapidly intensified in the following 24 h in both the Atlantic and east Pacific. When lightning density parameters are used as input to a discriminant analysis technique, results show that lightning information has the potential to improve the short-term prediction of tropical cyclone rapid intensity changes.

## 1. Introduction

Tropical cyclone intensity forecasts over the past few decades have improved considerably slower than track forecasts (e.g., Marks and Shay 1998; DeMaria et al. 2007). An especially difficult but important problem is the ability to forecast rapid intensity changes (RICs). In fact, improvement in RIC forecasting has been identified as the highest priority for research by the National Hurricane Center (NHC) and the Joint Typhoon Warning Center (Marks and Ferek 2011). Intensity changes involve complex interactions between a wide range of spatial scales in the atmosphere and ocean, as well as

physical processes such as surface energy exchanges, boundary layer turbulence, and cloud microphysics. Another difficulty is the lack of observations with adequate spatial and temporal resolution, especially near the storm center. Aircraft-based in situ and radar observations provide inner-core information, but are not available at all times, and cannot fully sample the three-dimensional wind and thermodynamic structure of a storm. Geostationary satellites provide measurements of visible and infrared radiation with high time and spatial resolution, but cloud cover typically prevents measurements below cloud top near the cyclone center. Passive and active microwave sensors from low-earth-orbiting (LEO) satellites provide information below the cloud top, including surface wind estimates and temperature and moisture profiles, but the horizontal and temporal resolution of these observations is limited. Thus,

*Corresponding author address:* Mark DeMaria, NOAA/NESDIS/ STAR, CIRA/CSU, 1375 Campus Delivery, Fort Collins, CO 80525. E-mail: demaria@cira.colostate.edu

tropical cyclone forecast models have incomplete information available for data assimilation and initialization.

Black and Hallett (1986) was one of the first studies to suggest that lightning observations might provide useful information about the hurricane inner-core region. Their study of aircraft observations of cloud microphysics from three Atlantic hurricanes showed that the simultaneous presence of ice and supercooled water, which is important for charge separation and lightning, was somewhat rare in the eyewall region. They suggested that remote lightning measurements would help locate these mixed phase regions. In a later study, Black and Hallett (1999) surveyed reports of electrical activity from a large sample of aircraft flights into tropical cyclones. Their results indicated that tropical cyclone lightning within 100 km of the storm center was somewhat rare and was usually associated with fairly strong updrafts ($>10$ m s$^{-1}$) in the mixed phase region above the freezing level. Although updrafts of 25 m s$^{-1}$ have been observed by aircraft (Black et al. 1994), the typical values in tropical cyclones are usually much weaker. For example, Jorgensen et al. (1985) showed that the 90th percentile of hurricane eyewall updraft speed was only about 4 m s$^{-1}$. Thus, lightning observations can also provide information about hurricane updraft strength, especially those on the very high end of the spectrum.

Thunderstorm lightning includes cloud-to-ground (CG) and intracloud (IC) strikes. Most estimates of the ratio of IC to CG strikes (often defined as $Z$) indicate that the majority of strikes are IC. For example, in a study of lightning activity in Brazil, De Souza et al. (2008) found $Z$ values ranging from 2 to 12. In a study over the continental United States, Boccippio et al. (2001) estimate a $Z$ value of about 3. Studies of thunderstorms over land indicate that total lightning (the sum of CG and IC strikes) is best correlated with updraft speed and convective structure (e.g., Reap and MacGorman 1989; Wiens et al. 2005). These findings indicate that total lightning measurements would provide the most information concerning the convective evolution and related intensity and structure changes of tropical cyclones.

Total lightning can be measured from ground-based lightning mapping arrays (LMAs), such as the Los Alamos Sferic Array (LASA) (Shao et al. 2006). The three-dimensional charge distribution can also be measured from LMAs, which allows the source height of the lightning to be estimated. Fierro et al. (2011) used LASA data to investigate the lightning activity in Hurricanes Rita and Katrina from the 2005 hurricane season while the cyclones were in the Gulf of Mexico. Results showed that the total lightning information was useful for monitoring the convective evolution of those storms. The results also showed that the periods of rapid intensification (RI) were

associated with an increase in the discharge heights of the IC lightning. This work again highlights the need for total lightning measurements in tropical cyclones. Unfortunately, the range of the LMAs is limited to a few hundred kilometers, so these systems are not well suited for statistical studies with large samples. A special class of IC lightning called narrow bipolar events (NBE) can be detected at longer ranges because of their characteristic large amplitudes (Fierro et al. 2011), but still cannot provide basinwide coverage.

Total lightning measurements can also be measured from satellites. The Optical Transient Detector (OTD) on a National Aeronautics and Space Administration (NASA) LEO satellite provided total lightning locations from 1995 to 2002 and the Lightning Imaging Sensor (LIS) on NASA's Tropical Rainfall Measuring Mission (TRMM) continues to provide total lightning measurements (Boccippio et al. 2002). Because the OTD and LIS only provide snapshots of lightning locations, they cannot be used to study the evolution of individual storms. However, they have been used to provide climatologies of the spatial coverage of total lightning (Christian et al. 2003) and have also been used in tropical cyclone studies through compositing approaches (Cecil et al. 2002).

Two exciting new developments that will provide total lightning measures over extended tropical cyclone regions are the ground-based Earth Networks Total Lightning Network (ENTLN; http://earthnetworks.com/Products/TotalLightningNetwork.aspx) and the space-based Geostationary Lightning Mapper (GLM), which will be on the next-generation Geostationary Operational Environmental Satellites (GOES) starting with GOES-R (www.goes-r.gov). The ENTLN uses a network of about 500 sensors that detect a broad range of frequencies to estimate total lightning locations. Some preliminary data are available in the Atlantic out to about 60°W from the 2010 and 2011 hurricane seasons. The GLM will provide near-continuous measures of total lightning locations over most of the area covered by GOES-East and -West, which includes most of the tropical cyclone regions of the Atlantic and eastern North Pacific basins. In addition, the GLM will have detection rates (70%–90%) that are comparable to or greater than those from ground-based systems. Part of the motivation for this study is to prepare for the GLM, which should become available by late 2015.

Because the ENTLN is a recent development and the GOES-R GLM is still several years away, most of the studies to date on tropical cyclone lightning have relied on ground-based systems, which primarily detect CG strikes. One of the earliest of these networks is the National Lightning Detection Network (NLDN), which has been available since the 1980s (Orville 2008). These

ground-based networks use very low-frequency (VLF) electromagnetic energy emitted during lightning discharges to estimate the time and location of CG lightning strikes. Although the detection efficiency of the NLDN decreases fairly rapidly outside of major land areas, these can also be used for tropical cyclone analysis for limited samples. Molinari et al. (1999) used NLDN data to show that the lightning density (LD; strikes per unit area and time) tends to have a bimodal structure as a function of radius from the storm center, with maxima near the eyewall region and in the rainband region (150–300-km radius) and a minimum in between. Corbosiero and Molinari (2003) extended that work to show a strong relationship between the environmental vertical wind shear and the azimuthal distribution of lightning, with a maximum in strikes on the downshear side of the storm.

More recently, Vaisala's Long Range Lightning Detection Network (LLDN; Pessi et al. 2009) and Global Lightning Dataset 360 (GLD360) (Demetriades et al. 2010) have been implemented. The LLDN extended the range of the NLDN to about 1000 km from the coast, and the GLD360 provides global coverage. Squires and Businger (2008) used the LLDN to perform cases studies of Hurricanes Katrina and Rita. Their study showed that lightning near the storm center tends to be much more transient than that in the rainband region, in agreement with the earlier studies such as those by Molinari et al. (1999) and Black and Hallett (1999). They also showed that large outbreaks of lightning occurred during the rapid intensification of those storms.

Because the GLD360 data provide global coverage, it is well suited for statistical studies of tropical cyclone lightning with large samples. However, this network was launched in September of 2009, so only a few hurricane seasons are currently available. The World Wide Lightning Location Network (WWLLN) operated by the University of Washington is another ground-based network that is well suited to tropical cyclone analysis because of its global coverage. The WWLLN data were established in the early 2000s (Lay et al. 2004; Rodger et al. 2006). As will be described in section 2, the WWLLN station coverage has improved considerably since its initial inception, and fairly uniform coverage is available back to at least 2005. For this reason, the WWLLN data will be used to investigate the relationships between lightning activity and tropical cyclone intensity changes for a large sample of Atlantic and eastern North Pacific tropical cyclones. In addition, the WWLLN detects some IC strikes (see section 2) so it is more representative of total lightning than the networks that only detect CG strikes.

The primary interest in this study is the relationship between lightning activity in tropical cyclones and intensity changes, especially rapid intensification and rapid weakening (RW). Using the simple argument that lightning is favored when the cloud updrafts are stronger in the mixed phase region (e.g., Black and Hallett 1999) it might be expected that increased lightning activity near the storm center would be correlated with short-term intensification. However, early studies with somewhat limited sample sizes did not reveal a clear relationship between lightning activity and tropical cyclone intensity changes (Molinari et al. 1999; Cecil et al. 2002). More recently, case studies of major hurricanes (MH) from the 2005 Atlantic hurricane season (Rita, Katrina, and Emily) by Squires and Businger (2008) and Thomas et al. (2010) showed that large increases in lightning near the storm center were observed slightly before and during periods of rapid intensification, but were also sometimes observed during weakening periods.

Price et al. (2009) examined lightning activity in a large sample of category-4 and -5 tropical cyclones around the globe using the WWLLN. His study showed a high correlation (0.82) between the lightning strikes in a large area around the storm and the maximum winds. Although the average lag between the peak lightning activity and maximum winds was about 30 h, the high correlations were obtained only after choosing the lag that maximized the correlation between lightning and maximum wind for each storm. The optimal lag ranged from 4 days before to 2 days after the peak wind was observed. When a fixed lag was used, the correlations were much lower. Kaplan and DeMaria (2003) showed that nearly all category-4 and -5 storms undergo at least one period of rapid intensification ($\geq$30 kt in 24 h, where 1 kt = 0.514 m s$^{-1}$) and, as described above, a number of studies have shown that tropical cyclone lightning is episodic with just a few short time periods with much higher lightning activity than during the rest of the storm. Thus, the results by Price et al. (2009) might simply be a result of these two observed characteristics, and do not conclusively establish a connection between lightning and intensification.

Abarca and Corbosiero (2011, hereafter A11) showed that for a sample of 24 Atlantic tropical cyclones, the inner-core lightning flash density is higher for cyclones that are intensifying than for those that are weakening. Their study used the WWLLN data and included the open ocean portion of the tracks of 2004–07 tropical cyclones that came within 400 km of the U.S. coastline during their lifetime. However, that study examined neither rapid intensity changes nor the relationship between lightning and future intensity changes.

In this study, the WWLLN flash densities of the entire lifetime of all Atlantic and eastern North Pacific tropical cyclones from 2005 to 2010 are examined to investigate

the relationships between lightning activity and intensity changes, with special emphasis on rapid intensity changes. For the remainder of this study we define rapid intensification as a 30-kt or more increase in the maximum sustained surface winds in 24 h and rapid weakening as a 20-kt or greater decrease in 24 h. Kaplan and DeMaria (2003) showed that a 24-h intensity increase of 30 kt is close to the 95th percentile of the long-term Atlantic intensity change distribution for cyclones over water. An examination of the Atlantic intensity changes from 1982 to 2010 for cyclones over water showed that a 24-h intensity decrease of 20 kt is close to the 5th percentile of the distribution.

The organization of the remainder of the paper is as follows: the data and analysis methods are described in section 2, the radial and temporal structures of the lightning activity are presented in section 3, the relationships between intensity changes and flash density are presented in section 4, and the potential for improving forecasts of rapid intensity changes using lightning information is described in section 5. Conclusions are provided in section 6.

## 2. Data and analysis methods

### a. Lightning data

The WWLLN provides estimates of the time and location of lightning strikes over most of the globe through analysis of VLF electromagnetic energy measured by a network of ground-based stations. These data were obtained from the University of Washington for the period 2005–10, where the data prior to 2008 were reprocessed using their upgraded (version 2) algorithm. As described by Rodger et al. (2008), the new algorithm increased the WWLLN detection efficiency by about 60%. Some data are also available back to 2003, but the station coverage was very limited during that time.

The location accuracy of the WWLLN has been estimated by modeling studies and comparisons with more accurate networks such as the LASA (Rodger et al. 2005; Jacobson et al. 2006). These studies indicate that the WWLLN location accuracy is about 15 km. As described below, the WWLLN data will be composited in a storm-relative coordinate system with radial bins no smaller than 50 km. The WWLLN location accuracy is acceptable for this purpose.

The WWLLN detection efficiency has been estimated in a number of studies through comparison with more accurate LMA networks over limited regions. As described by Lay et al. (2004), Jacobson et al. (2006), and Abarca et al. (2010, hereafter A10), the WWLLN detects CG and IC strokes with equal efficiency as long as their peak current is comparable. However, because the

WWLLN only detects strokes with large peak currents (>30 kA) and CG strikes tend to have larger peak currents than IC strikes, the WWLLN primarily detects CG strikes. In a recent evaluation of WWLLN, A10 estimated that the detection efficiency for WWLLN in 2008/09 over a domain that covered most of the continental United States and some adjacent ocean was 10.3% for CG, 4.8% for IC, and 6.2% for total lightning. Using the $Z$ value of 3 assumed in their study, about 58% of the WWLLN strikes are IC and 42% are CG. This estimate is larger than that in the study by Jacobson et al. (2006), which indicated that about 25% of the WWLLN strokes were IC. Although these results are fairly crude estimates, they do suggest that the WWLLN detects a nonnegligible fraction of IC lightning. A10 and A11 also concluded that although the overall WWLLN detection efficiency is fairly low, it can still measure the patterns of lightning strikes around tropical cyclones when compared to networks with much higher detection efficiencies. Figure 1 shows an example of the WWLLN lightning locations over a 6-h period for Hurricane Ike.

A10 and Rodger et al. (2008) have shown that WWLLN station coverage and detection efficiency have varied considerably over the period of this study. Therefore, a method to account for this variation is needed. As will be described below, the long-term global lightning density climatology estimated from OTD and LIS was used for this purpose. The properties of OTD and LIS are described by Boccippio et al. (2002). The flash detection accuracy is estimated to be about 90% so that they can provide an accurate estimate of the annual mean total lightning density over the tropics and subtropics. The annual mean lightning density on a 0.5° latitude–longitude grid was downloaded from the Goddard Space Flight Center web page, which included OTD data from 1995 to 2000 and LIS data from 1998 to 2005 in the climatology.

### b. Tropical cyclone data

The tropical cyclone tracks and maximum sustained 1-min surface winds (referred to as intensity) at 6-h intervals were obtained from the National Hurricane Center best-track dataset. The best track is determined from a postanalysis of all available information (Jarvinen and Davis 1984). Because the intensity is reported in knots rounded to the nearest 5, those units are used in this study. The life cycle of all tropical cyclones in the Atlantic tropical cyclone basin and combined eastern and central North Pacific tropical cyclone basins (i.e., out to the date line) from 2005–10 are included in the sample. In most years there are one or two storms that are classified as tropical cyclones but do not reach tropical storm intensity (34 kt or greater). These systems are sometimes referred to as unnamed depressions, and were
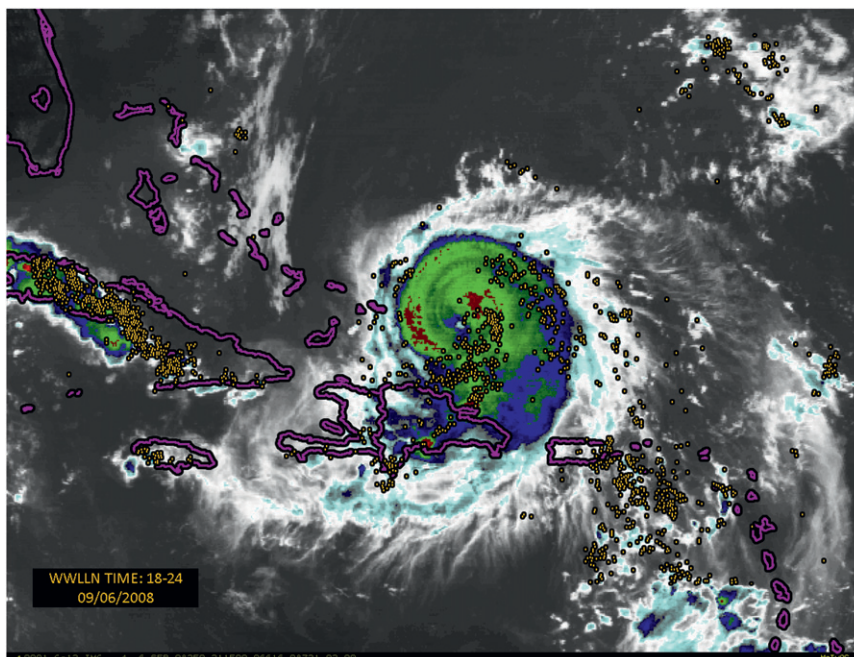
FIG. 1. The lightning locations (gold dots) from the WWLLN over a 6-h period centered at 2100 UTC 6 Sep 2008 on a color-enhanced GOES infrared image of Hurricane Ike. The red areas near the storm center indicate the coldest cloud tops.

included in the data sample. The Atlantic and eastern/central Pacific samples are considered separately. For simplicity the eastern/central Pacific cases are hereafter referred to as east Pacific.

Because the physical processes that govern tropical cyclone intensity changes of tropical cyclones after landfall are very different than those over the water, the sample is restricted to those cases where the center location is over water. Only relatively large landmasses are considered when excluding the land cases. Trinidad is the smallest island that is considered to be land in this study. The sample also excludes the extratropical stages of each storm because their structure is different than the tropical or subtropical systems. To calculate the time tendency of the intensity, the included best-track times were required to have a valid best-track point 12 h earlier and 24 h later. With these restrictions, the Atlantic sample includes 1245 six-hour periods from 81 tropical cyclones and the east Pacific sample includes 1297 six-hour periods from 91 tropical cyclones.

The best-track data were supplemented with an estimate of the vertical shear of the environmental horizontal wind and the sea surface temperature (SST). These were obtained from the developmental data for the Statistical Hurricane Intensity Prediction Scheme (SHIPS) (DeMaria 2010). The vertical wind shear is determined from the National Centers for Environmental Prediction (NCEP) Global Forecast System (GFS)

analysis by averaging the 200- and 850-hPa horizontal wind vectors over a circular area within a radius of 500 km from the storm center, and then taking the magnitude of the vector difference. The SST in the SHIPS dataset is estimated from the weekly Reynolds SST analysis at the center position of the storm.

### c. Data analysis methods

For comparison of lightning activity to intensity changes, the lightning strike locations were transformed to a storm-relative cylindrical coordinate system. The best-track center position was linearly interpolated to the time of each strike and then the radius and azimuth to that strike position was calculated. The area around the storm was then divided into eight radial intervals with a radial interval of 100 km. The lightning density was then calculated by counting the number of strikes in each 6-h period in each radial section and dividing by the area of that section. Similar to other studies (e.g., Squires and Businger 2008), the area from the 0- to 100-km radius is considered the inner-core region. The area from the 200- to 300-km radius is representative of the rainband region. The region from the 0- to 50-km radius is also examined, and will be referred to as the eyewall region. Because the interest is in future intensity changes, the lightning data for the 6 h before each best-track time were included in the LD calculation. The LD is reported in units of strikes per square kilometer per year,

TABLE 1. Adjustment factors needed to make the annual average WWLLN LD equal to that from the OTD/LIS climatology for each ocean basin and year.

| Year | Atlantic | East Pacific |
|------|----------|--------------|
| 2005 | 37.5 | 110.1 |
| 2006 | 24.1 | 31.1 |
| 2007 | 22.8 | 30.2 |
| 2008 | 16.7 | 15.2 |
| 2009 | 6.8 | 5.0 |
| 2010 | 5.0 | 5.7 |

consistent with the units of the climatological LD analyses that were used to normalize the data (e.g., Christian et al. 2003), as will be described below.

The annual mean lightning density climatology from OTD/LIS was used to account for time variability in the WWLLN detection efficiency. For this purpose it was assumed that variations in the lightning density averaged over large temporal and spatial areas are much smaller than the changes due to improvements in the WWLLN station coverage. With this assumption, the annual average lightning density was calculated for each year of the study over an Atlantic domain (0°–50°N, 100°–10°W) and an east Pacific domain (0°–40°N, 180°–100°W). These values were then compared to those from the annual lightning climatology over these same domains. Table 1 shows the adjustment factors needed to make to the WWLLN annual average LD equal that from the OTD/LIS climatology. Because the OTD/LIS climatology is for total lightning, the adjustment factors also correct for the low WWLLN detection efficiency and convert the values to total lightning densities in a mean sense. The year-to-year differences in the adjustment factors and the differences between the Atlantic and east Pacific values (especially in 2005) are believed to be due to increases in the number of stations in the WWLLN.

Table 1 shows that the total lightning detection rate (inverse of the adjustment factor) was only about 1%–3% in 2005, but increased to about 20% by 2010. A10

estimated that the WWLLN total lightning detection efficiency was 2.3% in 2006/07, which increased to 6.2% in 2008/09 over an area centered on the continental United States and adjacent waters. The area in A10 differs from the Atlantic and east Pacific domains in this study, but does include some overlap with each. Averaging the adjustment factors in Table 1 over both basins for 2006/07 and for 2008/09 gives detection rates of 3.7% and 10.9%, respectively. These detection rates are higher than those reported by A10 but are reasonably close given that the areas of comparison are not the same and contain much different fractions of land and water, and that the adjustment methods are very different. Also, the rate of improvement between the two time periods was 2.7 in A10, and 2.9 using the values from Table 1. This similarity provides some confidence that the normalization method used here adjusts for WWLLN improvements, at least in a relative sense. All of the LD measurements used in this study include the adjustment factors from Table 1, and are considered to be representative of total lightning.

## 3. Temporal variability and radial structure

To illustrate the temporal variability, Fig. 2 shows the Atlantic data sample of inner-core and rainband LD for all tropical cyclones in the sample plotted as a time series. All points for the same storm are plotted sequentially. The square root of the LD was plotted so that the structure of the lower values could be more easily seen. Neither time series indicates a significant trend, which provides confidence that the adjustment procedure was reasonable. The results show that the LD in the inner core and rainbands is extremely episodic, with long periods of very low activity interspersed with short periods of hyperactivity. As mentioned in the introduction, this episodic behavior is consistent with previous studies. The inner-core LD appears more variable than the rainband LD, consistent with the results of several other studies. As a quantitative measure of the temporal
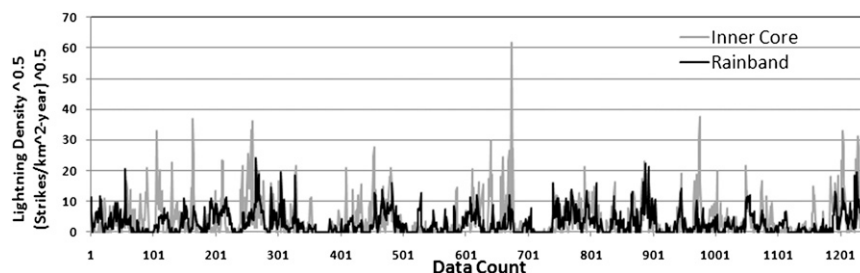


FIG. 2. The square root of the LD plotted as a sequential time series for all 6-h intervals for the Atlantic sample from 2005 to 2010.

TABLE 2. The 10 Atlantic cases with the largest inner-core LD. The max wind (Vmax), 24-h max wind change (dVmax), and environmental shear (Shear) are in kt and the SST is in °C.

| Name | Year | Time and date | LD | Vmax | dVmax | Lat (°N) | Lon (°W) | Shear | SST |
|------|------|---------------|-----|------|-------|----------|----------|-------|------|
| Noel | 2007 | 0600 UTC 1 Nov | 3792 | 50 | 20 | 23.4 | 78.3 | 18 | 28.8 |
| Ida | 2008 | 0000 UTC 9 Nov | 1399 | 90 | −30 | 23.0 | 86.5 | 28 | 28.1 |
| Mari | 2005 | 1200 UTC 30 Sep | 1369 | 50 | 15 | 24.4 | 53.1 | 7 | 28.5 |
| Philippe | 2005 | 0600 UTC 22 Sep | 1298 | 35 | 0 | 23.8 | 56.8 | 15 | 29.3 |
| Philippe | 2005 | 1200 UTC 22 Sep | 1110 | 45 | −10 | 19.9 | 57.0 | 24 | 29.6 |
| Richard | 2010 | 1200 UTC 22 Oct | 1093 | 35 | 15 | 15.8 | 81.0 | 13 | 27.7 |
| Irene | 2005 | 0600 UTC 8 Aug | 1074 | 35 | −5 | 21.8 | 48.3 | 17 | 29.4 |
| Thomas | 2010 | 1200 UTC 2 Nov | 960 | 40 | −10 | 13.5 | 72.5 | 15 | 28.6 |
| Ida | 2008 | 1200 UTC 8 Nov | 919 | 85 | −20 | 21.9 | 86.2 | 25 | 27.8 |
| Ingrid | 2007 | 0000 UTC 15 Sep | 881 | 35 | −5 | 15.9 | 51.2 | 20 | 29.2 |

variability, the standard deviation of the LD time series values in Fig. 2 (without the square root) was calculated. Results show that the inner-core standard deviation was 3.5 times larger than that of the rainband LD. Part of that difference might be due to the larger area of the rainband region. However, the LD standard deviation was also calculated for the area from 0 to 200 km, which is more comparable to that of the rainband region, and the standard deviation was still a factor of 1.5 larger. The results from the east Pacific (not shown) indicate similar behavior.

Table 2 shows the 10 Atlantic cases with the highest inner-core LD values. Only three of these cases intensified in the next 24 h, and none rapidly intensified. Eight of 10 were of tropical storm intensity (maximum winds less than 64 kt). The mean vertical shear and SST of the 2005–10 sample are 14 kt and 28.0°C, respectively. Table 2 shows that 8 of 10 cases had SSTs above the average and 8 of 10 had vertical shear above the average. Every case was equatorward of 25°. These results suggest that the largest inner-core LD occurs in Atlantic tropical cyclones at fairly low latitudes with high SSTs, but is also accompanied by above-average vertical shear. It is also interesting to note that all except one of the cases in Table 2 occurred in the latter half of the hurricane season. DeMaria et al. (2001) examined the relationship between vertical shear and thermodynamic instability in the tropical Atlantic. These results showed that the lowest vertical shear occurs fairly early in the season (early August), but the instability is at a maximum much later (late September/early October). The very large values of inner-core LD appear to favor the higher-shear, higher-instability environments.

To further examine the relationship between the inner-core LD and vertical shear, Fig. 3 shows a scatterplot of these two variables for the Atlantic sample. Again the square root of LD was used to highlight the lower values. The relationship between the inner-core LD and shear appears to be nonlinear, with two regimes. As the shear increases from low to moderate values, the LD increases. However, for very large values of shear, the LD generally decreases. The moderate values of shear may enhance updrafts near the storm by forcing asymmetries, as was shown by Corbosiero and Molinari (2003). However,
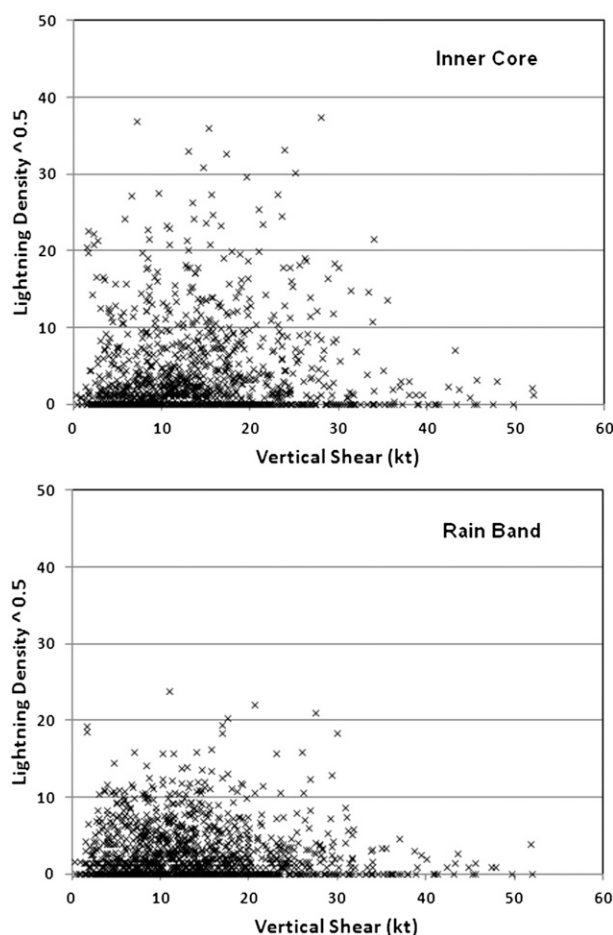


FIG. 3. Scatterplot of the vertical shear vs the square root of the LD for the Atlantic sample for the (top) inner-core and (bottom) rainband region.

for very large values of shear, the entire storm structure may become disrupted, resulting in dissipation and the lack of organized convection.

The nonlinear relationship between shear and inner-core LD is consistent with the modeling study by Davis et al. (2008), which examined the behavior of six Atlantic tropical cyclones interacting with vertical shear as they approached high latitudes and began extratropical transition. The model results showed that the environmental shear acted to tilt the vertical column of very high potential vorticity (PV) near the storm center, causing asymmetric vertical motion and convective structure. The cyclones counteracted the vertical shear through a procession of the tilt or by reformation of the low-level center in response to the asymmetric convection. The vertical mass flux in the simulations continued to increase during this process until the shear reached very high values. This increase and then decrease in model vertical mass flux is consistent with the increase in inner-core LD with increasing shear for moderate shear values and then a decrease for very large values of shear. The relationship between shear and the rainband LD does not appear to have the two-regime structure. Instead there appears to be a weak tendency for the LD to decrease with increasing shear. The rainband region is outside of the high-PV region and thus is not influenced by the PV tilt and associated vertical circulations. The general decrease in rainband LD in Fig. 3 is probably just due to the decreased instability that occurs at higher latitudes where the shear values are larger.

The inner-core and rainband lightning in Fig. 2 appear to be positively correlated, but the relationship between the two is not that strong. The correlation coefficient (without the square root used in Fig. 2) was only 0.13 for the Atlantic and 0.18 for the east Pacific. This result suggests that the lightning in the inner and outer parts of the cyclone is providing somewhat independent information on the storm structure and environment. This hypothesis will be examined in more detail in section 4.

Figure 4 shows the average LD as a function of radius for the Atlantic and east Pacific samples. The rainband region was subdivided into the eyewall region for this comparison, so the first two radial intervals in Fig. 4 are half the length of the remaining intervals. This figure shows that the average lightning density for the Atlantic is almost twice as large as that for the east Pacific. Both basins show a near-monotonic decrease in LD with radius. Previous studies (e.g., Molinari et al. 1999) have shown that there tends to be a local minimum in lightning activity between the inner-core region and the rainband region. This structure was observed in many individual cases, but does not appear in Fig. 4. This lack of a local minimum is due to the averaging of storms with
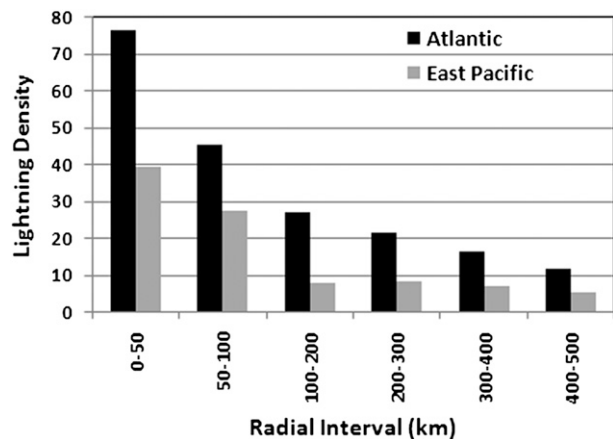


FIG. 4. The sample mean LD as a function of radius from the storm center for Atlantic and east Pacific tropical cyclones.

variable sizes, so that the high-lightning area of the inner core of large storms overlaps with the area between the rainbands and inner core of smaller storms. As will be shown below, a local minimum is observed when the cases are stratified by intensity.

The more rapid decrease in LD with radius for the east Pacific storms in Fig. 4 is consistent with the observation that east Pacific cyclones tend to be smaller than those in the Atlantic (Knaff et al. 2007). The LD is also smaller in the eyewall region for the east Pacific cases. It is possible that this is due to the generally lower vertical shear in that basin. It might also be due to atmospheric aerosol differences between the Atlantic and east Pacific. Khain et al. (2008) suggested that the increased availability of aerosols below cloud base increases the cloud supercooled water and ice concentrations, enhancing charge generation. The east Pacific aerosol concentration is less than that of the Atlantic (Sherwood 2002), which may be contributing to the lower LD for the east Pacific tropical cyclones.

A11 showed that inner-core LD was much larger for tropical depressions (TD) and tropical storms (TS) than for hurricanes. This relationship was also true in the rainband regions, but not as pronounced. A similar result was found in the case study comparisons of Samsury and Orville (1994). To further investigate these relationships with the larger data sample in this study, the Atlantic cases were stratified into four groups by maximum wind $v$: TD ($v < 34$ kt), TS ($34 \leq v < 64$ kt), nonmajor hurricanes (nMH; $64 \leq v \leq 94$ kt), and MH ($v > 94$ kt). Figure 5 shows that in the eyewall region (0–50 km), the LD is smaller for the TD cases, and about the same for the other intensity categories. It can also be seen that for the hurricanes, there is a local minimum in the $r = 50$–100-km region, especially for the MH cases. In A11, the 0–50- and 50–100-km radial intervals were
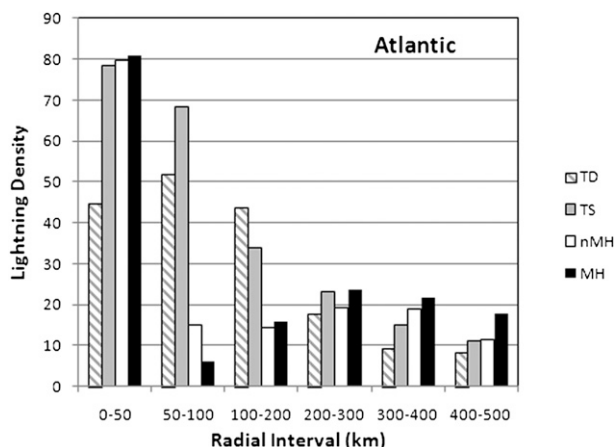
FIG. 5. The LD as a function of radius for the Atlantic sample stratified by the maximum winds (TD, TS, nMH, and MH). The sample sizes for the stratifications are 89, 668, 347, and 141, respectively.

combined. If those were combined in Fig. 5, and keeping in mind that the area of the second interval is 3 times larger than the first one, the TS and TD cases would have much larger LD values than the hurricane cases, consistent with the results of A11. However, the results in Fig. 5 indicate that some structure is lost when the data within the first 100 km from the storm center are combined.

The radial structure of the LD in Fig. 5 is consistent with observations of the inner-core convective structure of tropical cyclones, especially those with organized eyewall convection. Vigh et al. (2012) investigated a large sample of vortex data messages from routine aircraft reconnaissance flights. These messages include a radar-based estimate of the diameter of the inner edge of the eye if one is present. Their results show that the median eye diameter at the time when an eye was first observed is about 33 km (radius of 16.5 km), and the value does not vary very much from its initial value. Having a 10-km-wide eyewall and an outward slope where the eyewall radius can increase by up to about 50% from the lower to upper troposphere (Stern and Nolan 2009) indicates that nearly all of the eyewall convection will be within about 50 km. That is the width of the first bin in Fig. 5, which also shows the LD minimum outside of this radius for the hurricane cases. From the eyewall outward to about 100 km is an area that Cecil et al. (2002) called the inner rainband region. Using microwave satellite imagery and LIS data, they showed that this region is characterized by low precipitation, weak convection, and little lightning activity, consistent with the LD minimum in Fig. 5 for the hurricane cases. Outside of about 100 km, in a region they termed the outer rainband region, the convection signature was stronger and more lightning was observed, consistent with the secondary maximum in LD in Fig. 5 in the 200–300-km region.

The intensity stratification of the LD radial structure was also performed for the east Pacific sample, and the results were qualitatively similar to those shown in Fig. 5, although the local minimum at $r = 50$–$100$ km was less pronounced, probably because of the smaller size of the east Pacific tropical cyclones.

## 4. Lightning density and tropical cyclone intensity change

As described in section 1, the prediction of tropical cyclone intensity changes remains a difficult problem. For this reason, many previous studies of tropical cyclones have focused on the relationships between lightning and intensity changes, though with sometimes conflicting results. A11 stratified an Atlantic LD sample by intensification rate, and the intensifying systems did have large LD values in the inner core. There was no obvious difference in the rainband LD between the intensifying and nonintensifying cases. In that study, the intensification rate concurrent with the LD was examined. To have predictive value, the LD would need to be larger for cases that intensified after the time of the lightning measurements.

To examine the time lag relationships, the sample was stratified into three groups, where the maximum winds over a 6-h period decreased, remained constant, or increased. The cases where the maximum wind increased were then compared to those where it decreased. Of the 1245 cases, 22% were weakening and 37% were intensifying. This stratification was performed when the 6-h period of the intensity change was at the time of the 6-h period of the lightning data plus $-6$, 0, 6, . . . , 24 h. Figure 6 shows the LD for the weakening and intensifying cases as a function of the lead time between the data and the intensity change for the eyewall, inner-core, and rainband regions. For the eyewall and inner-core regions, the LD is larger for the intensifying cases than the weakening cases for lead times of $-6$ and 0 h, consistent with the results of A11. However, for the intensity changes 6 and 12 h after the lightning data, the relationships reverse, so that the weakening cases have higher LD than the intensifying cases. This result indicates that lightning activity near the storm center tends to occur during the intensification phase, but it is also an indicator that the intensification period is nearing its end. For the eyewall region, this relationship continues for lead times of 18 and 24 h, but reverses for the inner-core region at these longer lead times.

Figure 7 shows the LD stratified by intensity change for various lead times for the east Pacific sample. Of the 1297 cases, 24% were weakening and 36% were intensifying. Although the magnitudes are less, the structure
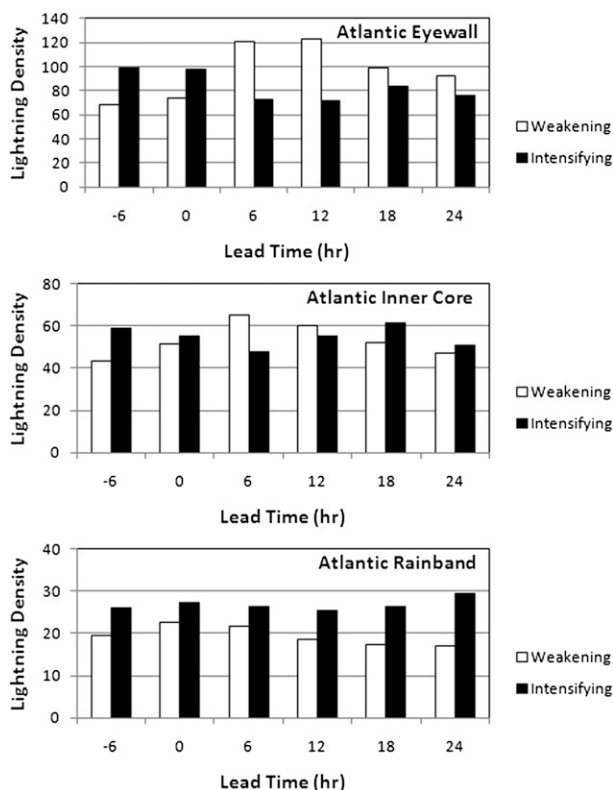
FIG. 6. The Atlantic LD for weakening and intensifying tropical cyclones, where the intensity change is estimated from the NHC best track at lead times of $-6, 0, \ldots, 24$ h relative to the 6-h interval of the lightning data. The results are for the (top) eyewall (0–50 km), (middle) inner-core (0–100 km), and (bottom) rainband (200–300 km) regions.



FIG. 7. As in Fig. 6, but for the east Pacific.

is remarkably similar to that for the Atlantic. The eyewall and inner-core LD are greater for the intensifying cases for lead times of $-6$ and 0 h, but the relationships reverse for lead times of 6 and 12 h. The rainband LD is greater for the intensifying cases at all lead times. Given that the east Pacific sample is completely independent of the Atlantic sample and has different size and aerosol properties, the similarity of the relationships indicates that these are robust results.

For the rainband region in Figs. 6 and 7, the LD is larger for the intensifying cases at all lead times out to 24 h. This suggests that the LD in the outer part of the storm might have more predictive information for intensity changes than that in the inner core.

One of most challenging aspects of intensity forecasting is the ability to anticipate rapid changes, either positive or negative. Figure 8 (top panel) shows the Atlantic LD as a function of radius for the rapid weakening, average intensity change (AIC), and rapid intensification cases. These stratifications of the Atlantic sample included 98, 1031, and 116 cases, respectively. The most obvious
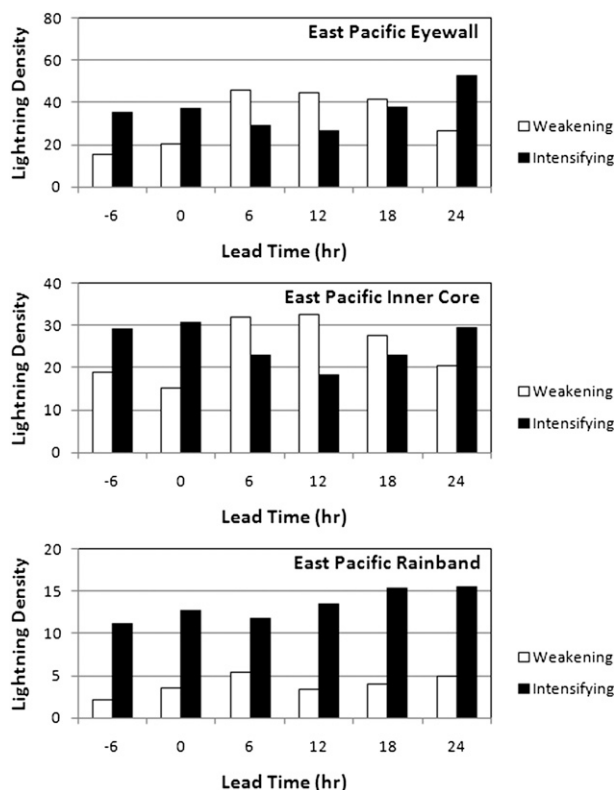
feature in Fig. 8 is that the eyewall LD is about 4 times greater for the RW cases than the RI cases. Again this is likely due to an intensification phase that is about to come to an abrupt end. Also evident in Fig. 8 for the Atlantic is that the rainband LD is about a factor of 2 larger for the RI cases than for the RW cases, again suggesting that the LD in the rainband region may be a good predictor of future intensity changes.

Figure 8 (bottom panel) shows the LD stratifications for the east Pacific. The number of RW, AIC, and RI cases for the east Pacific sample is 239, 961, and 97, respectively. A decrease in the maximum wind of 20 kt is about twice as common in the east Pacific than the Atlantic. This is because of the very strong SST gradients that occur in fairly low latitudes in the east Pacific. Because this is a different physical process than for the Atlantic storms, the eyewall LD stratifications are also very different. The largest eyewall LD occurs for the AIC cases, although the RW cases do have somewhat larger values than the RI cases. The LD in the rainband regions, however, is very similar to that for the Atlantic, with much higher values for the RI cases than the RW cases.

To help remove the effect of east Pacific storms that move over very cold water, the stratification shown in Fig. 8 was repeated but with only those cases where the
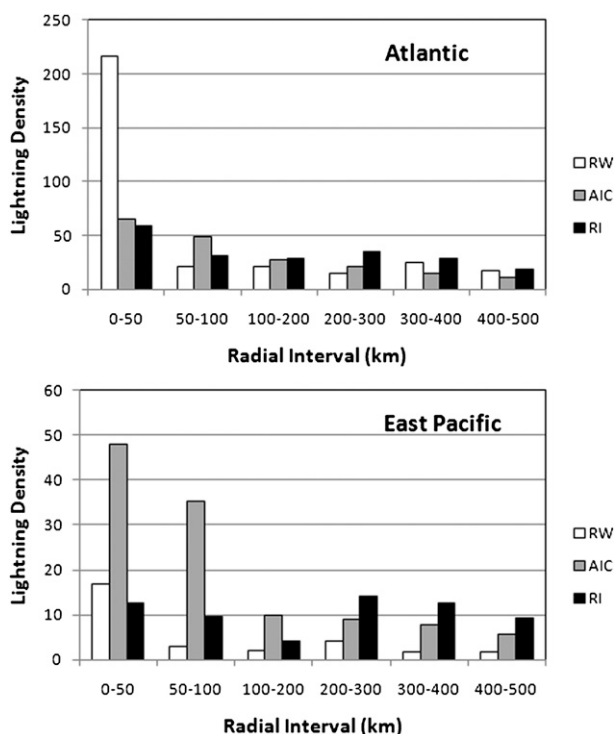
FIG. 8. Average LD for the RW, AIC, and RI cases as a function of radius for the (top) Atlantic and (bottom) east Pacific samples.

SST was at least 28°C. This sample included about half of the east Pacific cases. Results showed that for the warm SST cases, the eyewall LD for the RW cases was 2.8 times larger than that for the RI cases, similar to the Atlantic, although the LD for the AIC cases was still slightly larger than that for the RW cases. There was no qualitative change to the LD behavior in the rainband region for the east Pacific cases with warm SSTs.

The results shown in Figs. 6–8 indicate that the average eyewall LD is larger for intensifying tropical cyclones in the Atlantic and east Pacific, but this intensification phase will end within about 12 h. The results also show that the average LD in the rainband region is much larger for the RI cases, but the average eyewall LD is lower for the RI cases. Also, the average eyewall LD is larger for the RW cases, especially in the Atlantic. Some clues for the physical explanation of this behavior can be found in Figs. 2, 3. Figure 2 showed that the inner-core lightning and rainband lightning are not well correlated, indicating that they are modulated by different physical process. Figure 3 shows that the inner-core LD has a complex relationship with vertical shear, where shear increases the inner-core LD for moderate shear values but decreases it for large shear values. The rainband LD does not show this relationship. It is hypothesized that the interaction of the environmental shear with the inner-core PV is largely

responsible for the relationships between intensity changes and LD. As described in section 3, the Davis et al. (2008) study showed that the environmental vertical shear tilts the inner-core PV, resulting in asymmetric but more vigorous convection (increased mass flux). This enhanced asymmetric convection can lead to short-term intensification, but the negative effects of the vertical shear, and in some cases downdrafts and cold pools from the enhanced convection, halt the short-term intensification.

Although Davis et al. (2008) considered fairly high-latitude storms, this process can also occur in lower latitudes. For example, Molinari et al. (2006) showed that Hurricane Gabrielle (2001) interacted with an upper-level trough in the Gulf of Mexico, which increased the shear over the storm. The convection became very asymmetric and very strong, and resulted in a reformation of the center and short-term deepening. The CG lightning activity as measured by the NLDN was also very large during this process. However, the short-term intensification associated with the convective burst ended and the reformed center weakened before landfall along Florida's west coast. Many other cases of intense, asymmetric, convective outbreaks (sometimes called convective bursts) in tropical cyclones have been documented in the literature (e.g., Lyons and Keen 1994; Kelley and Halverson 2011). The rainband region, however, is outside of the core of high PV and thus is not impacted by the tilting and related vertical circulations induced by the interaction with shear. In that region, the LD is simply providing a measure of whether or not the storm environment is favorable for atmospheric convection.

Another physical process that may be responsible for the behavior of the inner-core and eyewall LD is the eyewall replacement cycle (Willoughby et al. 1982; Kossin and Sitkowski 2009). The updrafts in fairly symmetric hurricanes, even intense ones such as Hurricane Isabel (2003), are usually too weak to produce significant lightning activity (Demetriades and Holle 2005). However, as the eyewall contracts during a symmetric intensification process, the vertical velocity can increase enough to cause significant lightning activity as was seen for Hurricanes Emily, Katrina, and Rita during the 2005 season (Thomas et al. 2010). If the storm environment remains favorable, the inner eyewall collapses and is replaced by an outer eyewall, and the maximum wind decreases—sometime dramatically—during this process. Sitkowski et al. (2011) have shown using aircraft data that the average intensification phase of an eyewall replacement cyclone only lasts about 12 h. Thus, high eyewall LD would be correlated with short-term intensity increases (12 h or less), but longer-term weakening, consistent with Figs. 6, 7. However, Kossin and Sitkowski

(2009) showed using a large sample of microwave imagery that the probability of secondary eyewall formation is very low for tropical cyclones with maximum winds below about 80 kt, so eyewall replacement cycles are probably only a contributing factor to the relationship between eyewall LD and intensity changes.

## 5. The use of lightning for rapid intensity change forecasting

The results in section 4 show that the eyewall and rainband LD characteristics are very different for Atlantic tropical cyclones for the RW and RI cases. For the east Pacific storms, the rainband LD is also very different for the RW and RI cases. As a first test of the potential forecast utility of the lightning information, the operational rapid intensification index (RII) described by Kaplan et al. (2010) was generalized to include lightning input. The RII uses Fisher's linear discriminant analysis (LDA) technique (Wilks 2006) to identify the probability of rapid intensification in the following 24 h. The input includes a subset of the predictors used in the SHIPS model that are the most relevant to discriminating between the RI and non-RI cases, which are listed in Table 3. The maximum potential intensity in the SST potential discriminator is estimated from empirical relationships between observed intensities and SST as described in DeMaria and Kaplan (1999). The oceanic heat content (OHC) is estimated from satellite altimetry using the method described by Mainelli et al. (2008). Discriminators 4–6 are determined from the NCEP GFS model forecast averaged through 24 h. Discriminators 7 and 8 are calculated from GOES imagery at or prior to $t = 0$. Kaplan et al. (2010) have shown that the RII has skill relative to climatology and outperforms rapid intensity change forecasts from operational dynamical hurricane models.

To test the impact of the lightning input, discriminators 10 and 11 in Table 3 were added to those used in the operational RII. The square root of the LD was used instead of the LD itself because of the very episodic nature of the lightning data, where a few values are much larger than the rest of the sample. Also, the inner-core LD (0–100 km) was used instead of the eyewall LD (0–50 km) to provide a smoother input parameter and to account for storms with large eyes.

Because the lightning input also appears to have the potential to improve rapid weakening forecasts, the two-group RII algorithm was generalized to a three-group LDA (Wilks 2006). The discriminators for the operational RII were selected by comparing the differences in the sample means between the RI and non-RI cases. A similar procedure was applied for the RW and non-RW

TABLE 3. Discriminators used in the operational RII and the additional input for the experimental RIC algorithm.

| | Operational RII discriminators | |
| --- | --- | --- |
| No. | Name | Description |
| 1 | Persistence | Previous 12-h change in the max wind |
| 2 | SST potential | Max potential intensity − current intensity |
| 3 | OHC | Oceanic heat content at the storm center |
| 4 | Shear | 850–200-hPa vertical wind shear within 0–500-km radius |
| 5 | Divergence | 200-hPa divergence within 0–1000-km radius |
| 6 | RH | 850–700-hPa average RH within 200–800-km radius |
| 7 | IR asymmetry | GOES IR brightness temperature std dev |
| 8 | IR cold-cloud amount | % IR pixel counts colder than −30°C |
| | Additional discriminators for the experimental RIC algorithm | |
| 9 | Meridional wind | 200-hPa zonal wind in 0–500-km radius |
| 10 | Inner-core lightning | Square root of the 0–100-km LD |
| 11 | Rainband lightning | Square root of the 200–300-km LD |

cases and it was found that the 200-hPa meridional wind in the storm environment was a potentially useful discriminator, so that was added as an input parameter.

LDA determines the linear combination of the input variables that best distinguishes between groups. The procedure provides a weight for each input parameter for calculation of the discriminate function (the sum of the weights × the input parameters). The International Statistics and Mathematics Library (IMSL) software for Fisher's LDA was used to calculate the discriminate weights using the input parameters in Table 3 for the 2005–10 sample. The Atlantic and east Pacific samples were considered separately. For the two-group problem, the software provides two sets of weights for two discriminant functions. If the discriminant function corresponding to group 1 is the largest, that case is predicted to belong to group 1 and vice versa. For the operational RII the difference between the two discriminant functions is converted to a probability using the training data (dependent sample) in a simple nearest-neighbors approach. If the input parameters are normalized by dividing by the sample standard deviation of each, then the difference between the discriminant weights for each parameter provides a measure of its importance in the discrimination. For the three-group system, there are three sets of discriminant function differences that provide a measure of the importance of each input parameter for discriminating between groups 1 and 2, 2 and 3, and 1 and 3. To illustrate their relative importance, the difference of the normalized discriminant weights between the RI and RW cases was examined.

Figure 9 shows the magnitude difference in the normalized discriminant function weights between groups 3
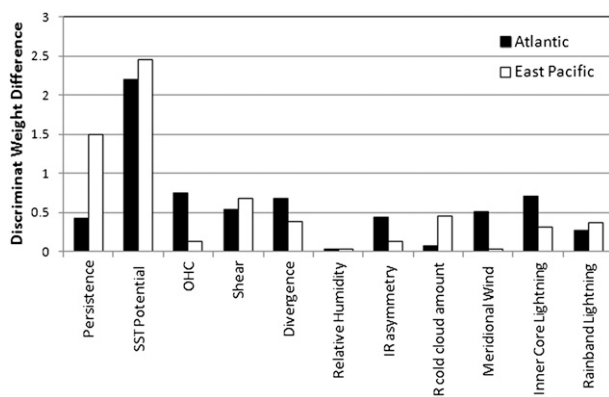
FIG. 9. The magnitude of the difference between the normalized discriminant weights for the RI and RW cases for the Atlantic and east Pacific samples.

(RI) and 1 (RW). The most important factor in both basins is the SST potential and the least important is the relative humidity. The magnitudes of the weight differences for the two lightning inputs are comparable to many of the other inputs included in the operational RII. This result suggests that the lightning input has the potential to improve forecasts of rapid intensity changes and is providing independent information relative to the parameters in the operational RII.

The sample size used to develop the operational RII is much larger than that used to determine the discriminant weights shown in Fig. 9 because the lightning data have not been available for as long as the other discriminators. The next step in the evaluation of the predictive value of the lightning input is to perform a test of the experimental algorithm on independent cases with and without the lightning input. This test is currently being performed as part of the GOES-R Proving Ground project at the National Hurricane Center, where the WWLLN data are being used as a proxy for the GLM. The evaluation of those forecasts will provide further information on the utility of the lightning data for forecasting rapid intensity changes of tropical cyclones.

## 6. Conclusions

A large sample of Atlantic and eastern North Pacific tropical cyclone cases (2005–10) was used to investigate the relationships between lightning activity in the storm core and its near environment and rapid intensity changes for storms over water. The lightning data were obtained from the ground-based World Wide Lightning Location Network (WWLLN) and a method was developed to correct for the improvements in the detection efficiency by comparison with a long-term lightning climatology from OTD/LIS. The lightning strikes over 6-h

periods centered on each tropical cyclone were used to calculate lightning density as a function of radius. The magnitude of the environmental wind shear from global model analyses and the SST are also included in the database.

The results from this study with a large data sample generally confirm those from previous studies: the average lightning density decreases with radius from the storm center, tropical storms have more lightning than hurricanes, intensifying storms have greater lightning density than weakening cyclones, and the lightning density for individual cyclones is very episodic. The results also show that Atlantic tropical cyclones have greater lightning density than east Pacific storms, which might be due to aerosol differences between the two basins. In contrast to some previous studies, the results show that the largest lightning density values are associated with sheared cyclones that are still over warm water, but do not intensify very much. The results also show that when the lightning density is compared with intensity changes in the subsequent 24 h, Atlantic cyclones that rapidly weaken in the following 24 h have a greater average inner-core lightning density than those that rapidly intensify. Thus, large inner-core lightning outbreaks are often a signal that an intensification phase is coming to an end. Conversely, the lightning density in the rainband regions (200–300 km) is higher for those cyclones that rapidly intensify in the following 24 h in both the Atlantic and east Pacific. It was hypothesized that the inner-core lightning structure is related to the interaction between vertical shear and the PV column associated with the storm circulation. Several studies (e.g., Davis et al. 2008) have shown that the PV column is tilted by the environmental shear, resulting in asymmetric but sometimes more intense convection. This can lead to short-term intensification, but that is often halted by the longer-term influence of the shear, and sometimes by downdrafts and cold pools associated with the intense asymmetric convection. Because the rainband region is outside of the high-PV region of the inner core, the LD in that region might provide a more direct measure of the convective instability of the storm environment. For stronger storms, secondary eyewall formation might also be a factor in explaining why inner-core lightning density is higher for tropical cyclones that rapidly weaken in the subsequent 24 h. These processes need to be investigated further using cases studies and model simulations.

The results of this study have a number of implications for tropical cyclone analysis and forecasting. When added to a linear discriminant analysis algorithm, the results showed that the lightning input influences the identification of rapidly intensifying and rapidly weakening

cases as much as many other parameters that are currently utilized in an operational rapid intensification index (Kaplan et al. 2010). Further testing with independent cases is needed to determine the impact on forecasting rapid intensity changes. An experimental version of the operational RII that also includes an estimate of the probability of rapid weakening is currently being tested in real time as part of the GOES-R Proving Ground project.

The results of the current and previous studies have shown that the lightning distribution is strongly related to characteristics of tropical cyclones and their environments. For example, there tends to be more lightning strikes in the downshear direction (Corbosiero and Molinari 2003). In the current study, the variations in the radial distributions of lightning density are related to the differences in the storm size, as revealed by the comparison of the Atlantic (i.e., larger storms) and east Pacific (i.e., smaller storms) samples. This study also demonstrated relationships between current and future intensity changes. These statistical relationships suggest that the lightning information has the potential to be used as input to data assimilation systems for hurricane model initialization. These capabilities would require the ability to relate lightning activity to variables that are predicted in the model such as updraft speed, supercooled water, and cloud ice. Several groups are currently developing these capabilities (e.g., McCaul et al. 2009; Fierro et al. 2011), which have the potential to provide information on tropical cyclones and their environments that is not normally available from other sources. The very episodic behavior of lightning activity described in this and other studies suggests that the relationships between lightning and other physical variables are very nonlinear, so the assimilation of this new data source is a challenging problem.

Finally, the WWLLN used in this study only detects a small fraction of the lightning, especially the IC strikes. Several studies with limited data samples show the importance of total lightning (IC and CG) (e.g., Fierro et al. 2011; Fierro and Reisner 2011). New ground- and space-based systems are becoming available that will provide total lightning measurements over large regions of the tropical oceans (the Earth Networks Total Lightning Network is currently being deployed and the GLM on GOES-R is planned for late 2015). These data will provide new insights into the relationships between total lightning and intensity changes.

## REFERENCES

Abarca, S. F., and K. L. Corbosiero, 2011: The World Wide Lightning Location Network and convective activity in tropical cyclones. *Mon. Wea. Rev.,* **139,** 175–191.

——, ——, and T. J. Galarneau Jr., 2010: An evaluation of the World Wide Lightning Location Network (WWLLN) using the National Lightning Detection Network (NLDN) as ground truth. *J. Geophys. Res.,* **115,** D18206, doi:10.1029/2009JD013411.

Black, R. A., and J. Hallett, 1986: Observations of the distribution of ice in hurricanes. *J. Atmos. Sci.,* **43,** 802–822.

——, and ——, 1999: Electrification in hurricanes. *J. Atmos. Sci.,* **56,** 2004–2028.

——, H. B. Bluestein, and M. L. Black, 1994: Unusually strong vertical motions in a Caribbean hurricane. *Mon. Wea. Rev.,* **122,** 2722–2739.

Boccippio, D. J., K. L. Cummins, H. J. Christian, and S. J. Goodman, 2001: Combined satellite- and surface-based estimation of the intracloud–cloud-to-ground lightning ratio over the continental United States. *Mon. Wea. Rev.,* **129,** 108–122.

——, W. J. Koshak, and R. J. Blakeslee, 2002: Performance assessment of the Optical Transient Detector and Lightning Imaging Sensor. Part I: Predicted diurnal variability. *J. Atmos. Oceanic Technol.,* **19,** 1318–1332.

Cecil, D. J., E. J. Zipser, and S. W. Nesbitt, 2002: Reflectivity, ice scattering, and lightning characteristics of hurricane eyewalls and rainbands. Part I: Quantitative description. *Mon. Wea. Rev.,* **130,** 769–784.

Christian, H. J., and Coauthors, 2003: Global frequency and distribution of lightning as observed from space by the Optical Transient Detector. *J. Geophys. Res.,* **108,** 4005, doi:10.1029/2002JD002347.

Corbosiero, K. L., and J. Molinari, 2003: The relationship between storm motion, vertical wind shear, and convective asymmetries in tropical cyclones. *J. Atmos. Sci.,* **60,** 366–376.

Davis, C. A., S. C. Jones, and M. Reimer, 2008: Hurricane vortex dynamics during Atlantic extratropical transition. *J. Atmos. Sci.,* **65,** 714–736.

DeMaria, M., 2010: Tropical cyclone intensity change predictability estimates using a statistical-dynamical model. Preprints, *29th Conf. on Hurricanes and Tropical Meteorology,* Tuscon, AZ, Amer. Meteor. Soc., 9C.5. [Available online at http://ams.confex.com/ams/29Hurricanes/techprogram/paper_167916.htm.]

——, and J. Kaplan, 1999: An updated statistical hurricane intensity prediction scheme (SHIPS) for the Atlantic and eastern North Pacific basins. *Wea. Forecasting,* **14,** 326–337.

——, J. A. Knaff, and B. H. Connell, 2001: A tropical cyclone genesis parameter for the tropical Atlantic. *Wea. Forecasting,* **16,** 219–233.

——, ——, and C. Sampson, 2007: Evaluation of long-term trends in tropical cyclone intensity forecasts. *Meteor. Atmos. Phys.,* **97,** 19–28.

Demetriades, N. W. S., and R. L. Holle, 2005: Long-range lightning applications for hurricane intensity. Preprints, *Conf. on Meteorological Applications of Lightning Data,* San Diego, CA, Amer. Meteor. Soc., P2.8. [Available online at http://ams.confex.com/ams/pdfpapers/84498.pdf.]

——, M. J. Murphy, and J. A. Cramer, 2010: Validation of Vaisala's Global Lightning Dataset (GLD360) over the continental United States. Preprints, *29th Conf. on Hurricanes and Tropical Meteorology,* Tuscon, AZ, Amer. Meteor. Soc., 16D.2.

[Available online at http://ams.confex.com/ams/29Hurricanes/techprogram/paper_168042.htm.]

De Souza, P. E., O. Pinto Jr., I. R. C. A. Pinto, N. J. Ferreira, and A. F. dos Santos, 2008: The intracloud/cloud-to-ground lightning ratio in Southeastern Brazil. *Atmos. Res.,* **91,** 491–499.

Fierro, A. O., and J. M. Reisner, 2011: High-resolution simulation of the electrification and lightning of Hurricane Rita during the period of rapid intensification. *J. Atmos. Sci.,* **68,** 477–494.

——, X.-M. Shao, T. Hamlin, J. M. Reisner, and J. Harlin, 2011: Evolution of eyewall convective events as indicated by intracloud and cloud-to-ground lightning activity during the rapid intensification of Hurricanes Rita and Katrina. *Mon. Wea. Rev.,* **139,** 1492–1504.

Jacobson, A. R., R. Holzworth, J. Harlin, R. Dowden, and E. Lay, 2006: Performance assessment of the World Wide Lightning Location Network (WWLLN), using the Los Alamos Sferic Array (LASA) as ground truth. *J. Atmos. Oceanic Technol.,* **23,** 1082–1092.

Jarvinen, B. R., and M. A. S. Davis, 1984: A tropical cyclone data tape for the North Atlantic basin, 1886-1983: Contents, limitations and uses. NOAA Tech. Memo. NWS NHC-22, 21 pp.

Jorgensen, D. P., E. J. Zipser, and M. A. LeMone, 1985: Vertical motions in intense hurricanes. *J. Atmos. Sci.,* **42,** 839–856.

Kaplan, J., and M. DeMaria, 2003: Large-scale characteristics of rapidly intensifying tropical cyclones in the North Atlantic basin. *Wea. Forecasting,* **18,** 1093–1108.

——, ——, and J. A. Knaff, 2010: A revised tropical cyclone rapid intensification index for the Atlantic and eastern North Pacific basins. *Wea. Forecasting,* **25,** 220–241.

Kelley, O. A., and J. B. Halverson, 2011: How much tropical cyclone intensification can result from the energy released inside of a convective burst? *J. Geophys. Res.,* **116,** D20118, doi:10.1029/2011JD015954.

Khain, A., N. Cohen, B. Lynn, and A. Pokrovsky, 2008: Possible aerosol effects on lightning activity and structure of hurricanes. *J. Atmos. Sci.,* **65,** 3652–3677.

Knaff, J. A., C. R. Sampson, M. DeMaria, T. P. Marchok, J. M. Gross, and C. J. McAdie, 2007: Statistical tropical cyclone wind radii prediction using climatology and persistence. *Wea. Forecasting,* **22,** 781–791.

Kossin, J. P., and M. Sitkowski, 2009: An objective model for identifying secondary eyewall formation in hurricanes. *Mon. Wea. Rev.,* **137,** 876–892.

Lay, E. H., R. H. Holzworth, C. J. Rodger, J. N. Thomas, O. Pinto Jr., and R. L. Dowden, 2004: WWLL global lightning detection system: Regional validation study in Brazil. *Geophys. Res. Lett.,* **31,** L03102, doi:10.1029/2003GL018882.

Lyons, W. A., and C. S. Keen, 1994: Observations of lightning in convective supercells within tropical storms and hurricanes. *Mon. Wea. Rev.,* **122,** 1897–1916.

Mainelli, M., M. DeMaria, L. K. Shay, and G. Goni, 2008: Application of oceanic heat content estimation to operational forecasting of recent Atlantic category-5 hurricanes. *Wea. Forecasting,* **23,** 3–16.

Marks, F. D., and L. K. Shay, 1998: Landfalling tropical cyclones: Forecast problems and associated research opportunities. *Bull. Amer. Meteor. Soc.,* **79,** 305–323.

Marks, F., and R. Ferek, 2011: Comparison of the 2008 and 2010 snapshots of tropical cyclone R&D. *Proc. 65th Interdepartmental Hurricane Conf.,* Miami, FL, Office of the Federal Coordinator for Meteorology, 24 pp. [Available online at http://www.ofcm.gov/ihc11/linking_file_ihc11.htm.]

McCaul, E. W., S. J. Goodman, K. M. LaCasse, and D. J. Cecil, 2009: Forecasting lightning threat using cloud-resolving model simulations. *Wea. Forecasting,* **24,** 709–729.

Molinari, J., P. Moore, and V. Idone, 1999: Convective structure of hurricanes revealed by lightning locations. *Mon. Wea. Rev.,* **127,** 520–534.

——, P. Dodge, D. Vollaro, K. L. Corbosiero, and F. Marks Jr., 2006: Mesoscale aspects of the downshear reformation of a tropical cyclone. *J. Atmos. Sci.,* **63,** 341–354.

Orville, R. E., 2008: Development of the national lightning detection network. *Bull. Amer. Meteor. Soc.,* **89,** 180–190.

Pessi, A. T., S. Businger, K. L. Cummins, N. W. Demetriades, M. Murphy, and B. Pifer, 2009: Development of a long-range lightning detection network for the Pacific: Construction, calibration, and performance. *J. Atmos. Oceanic Technol.,* **26,** 145–166.

Price, C., M. Asfur, and Y. Yair, 2009: Maximum hurricane intensity preceded by increase in lightning frequency. *Nat. Geosci.,* **2,** 329–332, doi:10.1038/NGEO477.

Reap, R. M., and D. R. MacGorman, 1989: Cloud-to-ground lightning: Climatological characteristics and relationships to model fields, radar observations, and severe local storms. *Mon. Wea. Rev.,* **117,** 518–535.

Rodger, C. J., J. B. Brundell, and R. L. Dowden, 2005: Location accuracy of VLF World Wide Lightning Location (WWLL) network: Post-algorithm upgrade. *Ann. Geophys.,* **23,** 277–290.

——, S. Werner, J. B. Brundell, E. H. Lay, N. R. Thompson, R. H. Holzworth, and R. L. Dowden, 2006: Detection efficiency of the VLF World-Wide Lightning Location Network (WWLLN): Initial case study. *Ann. Geophys.,* **24,** 3197–3214.

——, J. B. Brundell, R. H. Holzworth, and E. H. Lay, 2008: Growing detection efficiency of the World Wide Lightning Location Network. *Proc. Conf. on Coupling of Thunderstorms and Lightning Discharges to Near-Earth Space,* Vol. 1118, Corte, France, American Institute of Physics, 15–20.

Samsury, C. E., and R. E. Orville, 1994: Cloud-to-ground lightning in tropical cyclones: A study of Hugo (1989) and Jerry (1989). *Mon. Wea. Rev.,* **122,** 1887–1896.

Shao, X. M., M. Stanley, A. Regan, J. Harlin, M. Pongratz, and M. Stock, 2006: Total lightning observations with the new and improved Los Alamos Sferic Array (LASA). *J. Atmos. Oceanic Technol.,* **23,** 1273–1288.

Sherwood, S. C., 2002: Aerosols and ice particle size in tropical cumulonimbus. *J. Climate,* **15,** 1051–1063.

Sitkowski, M., J. P. Kossin, and C. M. Rozoff, 2011: Intensity and structure changes during hurricane eyewall replacement cycles. *Mon. Wea. Rev.,* **139,** 3829–3847.

Squires, K., and S. Businger, 2008: The morphology of eyewall lightning outbreaks in two category-5 hurricanes. *Mon. Wea. Rev.,* **136,** 1706–1726.

Stern, D. P., and D. S. Nolan, 2009: Reexamining the vertical structure of tangential winds in tropical cyclones: Observations and theory. *J. Atmos. Sci.,* **66,** 3579–3600.

Thomas, J. N., N. N. Solorzano, S. A. Cummer, and R. H. Holzworth, 2010: Polarity and energetics of inner core lightning in three intense North Atlantic hurricanes. *J. Geophys. Res.,* **115,** A00E15, doi:10.1029/2009JA014777.

Vigh, J. L., J. A. Knaff, and W. H. Schubert, 2012: A climatology of hurricane eye formation. *Mon. Wea. Rev.,* **140,** 1405–1426.

Wiens, K. C., S. A. Rutledge, and S. A. Tessendorf, 2005: The 29 June 2000 supercell observed during STEPS. Part II: Lightning and charge structure. *J. Atmos. Sci.,* **62,** 4151–4177.

Wilks, D. S., 2006: *Statistical Methods in the Atmospheric Sciences.* 2nd ed. Elsevier, 627 pp.

Willoughby, H. E., J. A. Clos, and M. Shoreibah, 1982: Concentric eye walls, secondary wind maxima, and the evolution of the hurricane vortex. *J. Atmos. Sci.,* **39,** 395–411.